Proceedings of the 10o Brazilian Congress of Thermal Sciences and Engineering -- ENCIT 2004
Braz. Soc. of Mechanical Sciences and Engineering -- ABCM, Rio de Janeiro, Brazil, Nov. 29 -- Dec. 03, 2004

ANALYSIS OF THE COMBUSTION WITH EXCESS ENTHALPY IN POROUS MEDIA

Fernando Marcelo Pereira
Department of Mechanical Engineering
Federal University of Santa Catarina
Florianópolis - SC
fernando@cet.ufsc.br

Amir Antonio Martins Oliveira
Department of Mechanical Engineering
Federal University of Santa Catarina
Florianópolis - SC
amirol@emc.ufsc.br

Abstract. The premixed gas combustion within an inert porous media allows the gas temperature inside the porous matrix to achieve temperatures higher than the adiabatic flame temperature based on the gas inlet condition. This is called superadiabatic combustion. This work analyses numerically the excess enthalpy in laminar free flames and in flames within porous media in order to estimate the amount of excess temperature originated by the presence of the porous matrix and the factors that affect it. The analysis is based on the excess enthalpy function previously defined in the literature, applied to the non-dimensional volume-averaged equations for the combustion within an inert porous medium. A two-medium treatment is used to model the non-equilibrium between the gas and the solid phases. The excess temperature is shown to be a function of the gas Lewis number, the ratio of the solid- and the gas-phasic effective conductivities and the porosity of the medium. By directly comparing the two-medium results with the results obtained for a laminar free flame, the effect of each of these variables is assessed.

Keywords. *superadiabatic combustion, porous media, excess enthalpy, thermal and chemical non-equilibrium.*

1. Introduction

The thermal non-equilibrium characteristic of the premixed gas combustion within an inert porous media results in enhanced combustion which can be used to augment the local heat generation or to burn fuel lean mixtures. This non-equilibrium is basically a result of the large ratio between the solid thermal conductivity and the gas thermal conductivity, which can be several orders of magnitude larger than one, and of the finite interfacial heat transfer between the phases. This effect is also noted in the increase of the laminar flame speed when compared to free flames. This behavior has been known for a long time (Hardesty and Weimberg, 1974) and has found several applications in engineering, where the thermal and chemical non-equilibrium comes to the advantage of the design engineer (Oliveira and Kaviany, 2001).

The usual explanation for the excess temperature is based on the enhanced heat transfer by conduction through the solid compared to the gas phase. The intramedium radiation between the solid particles can also play an important role in the heat transfer between the hot and the cold regions of the flame. This larger energy transfer through the solid matrix cause a substantial preheating of the gas phase, i.e., a heat recirculation (Howell et al., 1996). The heat recirculation adds to the energy released by combustion resulting in local temperatures in excess of the adiabatic flame temperature for the gas phase, which is called superadiabatic combustion (Echigo et al., 1991). This high temperature in the reaction region increases the reaction rate and allows for combustion of low heat content gas mixtures whose stoichiometric ratio lies under the flammability limit in laminar free flames.

For gas Lewis numbers different from one, the laminar premixed free flames also present either an excess enthalpy or a defect enthalpy when compared to the unity Lewis number flames. The excess enthalpy, however, may not lead to excess temperatures. Our goal in this work is to analyze the energy concentration in the reaction zone of premixed stationary flames within inert porous media comparing it to the free flame premixed combustion in order to clarify the conditions necessary to achieve excess temperatures. It will be seen that the heat recirculation effect is a consequence of the combined effect of the modified Lewis number, the thermal conductivity ratio between the phases and the porosity of the solid matrix.

In the following, the excess temperature for both laminar free flames and flames within a porous medium are discussed based on the literature on experimental and theoretical work.

2. The Excess Temperature

The energy concentration in the flame zone in premixed combustion, also known as excess enthalpy premixed combustion, has been investigated by several authors as a way of enhancing combustion to augment the local amount of heat generated or to allow for the combustion of low grade fuels (Hardesty and Weinberg, 1974; Howell et al., 1996; Babkin et al., 2003; and others). Babkin et al. (2003) show that excess enthalpy flames can exist in various systems and combustion regimes. The total enthalpy is defined here as in the usual way in premixed flame theory (William, 1985). Their work lists various mechanisms that lead to energy concentration in the combustion front or, for example, mass diffusion in cellular flames for Le < 1, heat recuperation from the products in regenerative burners, dilution of reactants with exhaust gases in tunneling burners, heat recirculation through a solid matrix in porous burners, etc..

Even in free laminar flat flames it is possible to observe a certain degree of excess enthalpy. This occurs when the thermal diffusivity of the gas mixture α_g exceeds the mass diffusivity D, i.e., when the molecular Lewis number is greater than unit. Wichman and Vance (1997), studying flame annihilation, have discussed the excess enthalpy in free flat flames. They calculated an excess enthalpy function H, both analytically using a thin flame asymptotic and numerically, and have showed the effect of the Lewis number on the H distribution along the flame, on the maximum value of H and its location. They showed that the excess enthalpy increases with the increase of the Lewis number. However, there is no indication when this excess enthalpy would produce temperatures above the adiabatic temperature.

The combustion in porous media has been widely investigated in the last two decades (for example, see the reviews by Echigo, 1991, Howell et al., 1996 and Oliveira e Kaviany, 2001) as a way of producing and stabilizing an excess enthalpy flame. These works have shown theoretically and experimentally that the non-equilibrium between the phases in the reaction region can lead the gas temperature to a superadiabatic condition, i.e., the local gas temperature in the flame zone may exceed the adiabatic flame temperature for the inlet free stream conditions. The amount of this excess temperature varies with the geometric (including the size) and thermo physical properties of the medium (mainly, its thermal conductivity and optical thickness), the fuel and equivalence ratio, the gas velocity and the strength of the heat loss, both volumetrically and at the inlet and outlet ends. The experimental measurement of the excess temperature is always subjected to all the errors inherent to the temperature measurement in gas phase flames (mainly radiation and catalytic reaction) increase by the difficulties in realizing this measurement within a confined medium with tortuous, at most, millimeter sized, pores. Usually, the temperature probes come into contact with the solid phase, and the measured temperature is in fact some sort of gas-solid averaged temperature. Some strategies to minimize these measurement errors have been used by Mittal et al. (1997) and Min and Shin (1991). The theoretical prediction has relied in the use of volume-averaged models, coupled either with simple or detailed chemical kinetics, including the use either of a diffusive approximation or the solution of the RTE equation for the intra-medium thermal radiation, solved for an infinite of finite length porous media, usually subjected to radiation boundary conditions at both ends. One-dimensional or axi-symmetric two-dimensional analysis, usually with no other form of volumetric heat generation or loss, have been performed.

Sahraoui and Kaviany (1994) solved the one-medium model (i.e., a model that assumes local thermal equilibrium between the solid and the gas phases - $T_g=T_s=T$), the two-medium model (which allow for surface heat transfer between the phases) - both are volume-averaged models - and the pointwise local conservation equations (i.e., the differential conservation equations applied to the gas channel and the solid phase particles) for a periodic medium composed of square particles assuming gas phase and effective Lewis number equal to unit and assuming an infinitely long medium. The solid-gas heat transfer coefficient was obtained from the pointwise solution, averaged on the particle surface, and used in the two-medium model. A one-step global chemical kinetic mechanism was used, with the parameters chosen to match measured values of flame speed for methane-air flames. For $\lambda_s/\lambda_g = 100$, equivalence ratio $\Phi=1$ and a porosity $\varepsilon=0.9$, they obtained local excess temperatures of 252 K solving the pointwise local equations and 43 K solving the two-medium model. The one-medium model, although not intrinsically able to predict superadiabatic temperatures, predicted the flame thickness and flame velocity fairly well. We could argue that, as a parallel to a free flame, the one-medium model should be able to predict excess enthalpies, if the authors had allowed for larger Lewis numbers. For the two-medium and the pointwise model an increase in the medium conductivity for the solid phase increases the axial heat conductivity and causes an augmentation of the excess temperature.

Boshoff-Mostert and Viljoen (1996) solved a one-dimensional, two medium model neglecting the mass diffusion ($Le \to \infty$) using an asymptotic expansion method for a finite porous medium with zero heat losses at both ends. The porous medium is divided into three regions, a preheating, a reaction and a post-reaction region, the high activation energy asymptotic is used and the solution provides the flame location and the maximum temperature as a function of the steady-state laminar flame speed. They show that the excess temperature increases with the increase in flame speed and the increase is steeper for lower Φ. The maximum temperature in the reaction region approaches the adiabatic flame temperature for low speeds. There are two stable flame positions, one near the inlet and another near the outlet. For each Φ there is a lower and an upper limit for the flame speed and the stability range increases as Φ increases.

In both these models a diffusive approximation for the intramedium thermal radiation was used. Chen et al. (1987) studied the effect of radiation on the structure of premixed flames within a highly porous inert media solving the RTE equation. They solved a one medium model neglecting scattering and heat loss by radiation in both ends of the burner. They fixed the flame location inside the porous medium and even assuming thermal equilibrium between the phases (the one-medium model) they were able to detect a superadiabatic temperature. We could argue that this occurred only because the solution attempted to satisfy the energy balance wherever the flame location was fixed. Nonetheless, they showed that the intramedium radiation increases the radiation output and the flow preheating.

Hsu and Matthews (1993) solved a two-medium model for a finite porous media with radiation exchange in both ends of the burner and using a multi-step chemistry. Their results showed that the multi-step chemistry reduces the excess temperature when compared to a global, single-step reaction mechanism. They explain this by the dissociation of combustion species, which reduce the flame temperature. Nonetheless, the excess temperature, although smaller, remained in their calculations. Zhou and Pereira 1998, solving a similar problem without heat loss, reached the same results and argued that the multi-step mechanism spread the energy release over a broader flame front rather than a narrow flame front predicted by the global reaction, thus reducing the amount of excess temperature.

In this work, we first write the one-dimensional conservation equations for energy and chemical species using a two-medium model based on Sahraoui and Kaviany (1994). The equations are scalled using appropriate nondimensional parameters and the magnitude of each parameter for the premixed flame in porous media used in the applications is discussed. Then, we theoretically discuss the excess enthalpy in free and stationary laminar flames within an inert porous media and analyze the necessary conditions for the existence of superadiabatic temperatures.

3. Analysis

3.1. Free Flame Combustion

A one-dimensional model for the conservation of energy and species is presented below. The mass conservation implies that $\rho_n u_n$ is constant for the one-dimensional flow with ρ_n and u_n being respectively the gas density and the gas velocity far upstream from the flame. For a steady state, stationary flame, the laminar flame speed S_L is equal to u_n. The specific heat c_p, the thermal conductivity and the product ρD (density times mass diffusivity) are assumed uniform along the flame. As the pressure across the flame front is approximately uniform the momentum equation is neglected. A single-step, first-order in the fuel concentration and zeroth-order in the oxidant concentration, Arrhenius reaction rate is adopted. The equations are:

$$\rho_n u_n \frac{dY_F}{dx} = \rho D \frac{d^2 Y_F}{dx^2} - w \qquad (1)$$

$$\rho_n u_n c_p \frac{dT_g}{dx} = \lambda_g \frac{d^2 T_g}{dx^2} + wQ \qquad (2)$$

$$w = A T_g^a \nu_F \rho Y_F \exp\left(\frac{-T_i}{T_g}\right) \qquad (3)$$

where Q is the heat of reaction, T_i is the ignition temperature that is equal to $\Delta E_a/R_g$ with ΔE_a being the activation energy and R_g the universal gas constant. A first order, single step reaction, although not accurate, allows for a simple analysis and will be used here.

Defining the nondimensional fuel mass fraction, temperature and spatial coordinate as

$$y = \frac{Y_F}{Y_{F,n}}, \quad \theta = \frac{c_p (T - Tn)}{Y_{F,n} Q} = \frac{T - T_n}{T_r - T_n}, \quad \zeta = \int_0^x \frac{\rho_n u_n c_p}{\lambda_g} dx \qquad (4)$$

The nondimensional equations transformed to the spatial coordinate ζ are (Williams, 1985):

$$\frac{dy}{d\zeta} = \left(\frac{1}{Le}\right) \frac{d^2 y}{d\zeta^2} - DaW \qquad (5)$$

$$\frac{d\theta_g}{d\zeta} = \frac{d^2 \theta_g}{d\zeta^2} + DaW \qquad (6)$$

where the nondimensional parameters appearing in the conservation equations are:

$$Le = \frac{\lambda_g}{\rho c_p D}, \qquad Da = \frac{A_0 \nu_F T_g^a \rho e^{\frac{-\beta}{\alpha}} \lambda_g}{\rho_n^2 u_n^2 c_p}, \qquad W = y \exp\left[\frac{-\beta(1-\theta_g)}{1-\alpha(1-\theta_g)}\right],$$

$$\beta = \alpha \frac{E_a}{R_g T_r} = \frac{E_a (T_r - T_n)}{R_g T_r^2}, \qquad \alpha = \frac{Q Y_{F,n}}{c_p T_r} = \frac{T_r - T_n}{T_r} \qquad (7)$$

where Da is the Damköhler number, W is nondimensional reaction rate, α is the enthalpy ratio and β is the Zeldovich number. The parameters Le, β and α are constants that depend upon the initial conditions and the constant properties assumed in the model. The Damköhler number is assumed to be independent of θ_g (Williams, 1985).

Summing Equations (5) and (6) up we find:

$$\frac{d\left(y+\theta_g\right)}{d\zeta} = \frac{d^2}{d\zeta^2}\left(\frac{y}{Le}+\theta_g\right) \tag{8}$$

The overall energy balance $c_p(T-T_n) = Q(Y_{F,n}-Y_F)$ is nondimensionalized to give $y + \theta_g = 1$, then, one can define a new variable $H = y + \theta_g - 1$, called excess enthalpy function. This function accounts for the total enthalpy of the gas, including the thermal and chemical enthalpies. From the definition of H, Eq. (8) is rewritten as:

$$\frac{dH}{d\zeta} = \frac{d^2H}{d\zeta^2} + \left(\frac{1}{Le}-1\right)\frac{d^2y}{d\zeta^2} \tag{9}$$

For a unit Lewis number, H is equal to zero anywhere in the flame. Equation 9 states that when $Le \neq 1$, the second term in the right hand side becomes a positive or a negative source term depending on the sign for $d^2y/d\zeta^2$ and H is no longer conserved. Wichman and Vance (1997), using a thin flame asymptotic, showed that in an adiabatic laminar free flame with $Le < 1$ this equation would give a defect enthalpy ($H < 0$) and for $Le > 1$ it would give an excess enthalpy ($H > 0$). It is important to note that an excess enthalpy does not mean an excess temperature because the excess enthalpy can be originated by an excess fuel concentration in the preheating zone. Even when there is a local excess temperature, it may not be above the adiabatic flame temperature, depending on the local values of fuel concentration.

3.2. Combustion in Porous Media

Two Equations Model:

A one-dimensional, two-medium model for the conservation of mass, gas phase energy, solid phase energy and species are written following Sahraoui and Kaviany (1994). The gas and solid radiation and the dispersion effects are neglected. For a highly porous ($\varepsilon > 0.75$), large pores ($D_p > 0.1$ mm) porous media, the pressure along the porous medium is approximately uniform, and the momentum equation becomes trivial. The thermal conductivities (λ_g for the gas and λ_s for the solid) and the mass diffusivity D are effective properties in the respective phase (i.e., include the pore channel variable area and tortuosity effects). The steady state, volume-averaged energy conservation equations (omitting for simplicity the volume-averaging notation) then become:

$$\varepsilon\rho_n u_n c_p \frac{dT_g}{dx} = \varepsilon\lambda_g \frac{d^2T_g}{dx^2} + \varepsilon wQ + h_v\left(T_s - T_g\right) \tag{10}$$

$$0 = \left(1-\varepsilon\right)\lambda_s \frac{d^2T_s}{dx^2} - h_v\left(T_s - T_g\right) \tag{11}$$

where ε is the porosity of the solid matrix, $h_v = S_{gs}h$, is the volumetric convection coefficient, S_{gs} is the interfacial specific area between the solid and the gas phases (m^2/m^3), $h = Nu\lambda_{s,m}/D_p$ is the local convection coefficient with, Nu, D_p and $\lambda_{s,m}$ being respectively the averaged Nusselt number for a fully developed flow through a porous medium, the mean pore diameter of the solid matrix and the molecular thermal conductivity of the gas phase. The nondimensional equations are:

$$\varepsilon\frac{dy}{d\zeta} = \varepsilon\left(\frac{1}{Le_s}\right)\frac{d^2y}{d\zeta^2} - \varepsilon DaW \tag{12}$$

$$\varepsilon\frac{d\theta_g}{d\zeta} = \varepsilon\left(\frac{1}{\Gamma_s}\right)\frac{d^2\theta_g}{d\zeta^2} + \varepsilon DaW + N\left(\theta_s - \theta_g\right) \tag{13}$$

$$0 = \left(1-\varepsilon\right)\frac{d^2\theta_s}{d\zeta^2} - N\left(\theta_s - \theta_g\right) \tag{14}$$

where the spatial coordinate is now based on the solid conductivity. The new nondimensional parameters appearing in the volume-averaged conservation equations are:

$$\mathrm{Le}_s = \mathrm{Le}\Gamma_s \qquad \Gamma_s = \frac{\lambda_s}{\lambda_g}, \qquad N = \frac{\lambda_s h_v}{\left(\rho_n u_n c_p\right)^2} \tag{15}$$

In these equations, Le_s is the Lewis number based on the solid conductivity, Γ_s is the ratio between the solid and gas conductivities and N is the interfacial heat transfer parameter. The parameter N is assumed to be independent of θ_g.

As for the laminar free flame, the sum of Eqs. (12), (13) and (14) leads to:

$$\frac{d\left(y+\theta_g\right)}{d\zeta} = \frac{d^2}{d\zeta^2}\left[\frac{1}{\mathrm{Le}_s} y + \frac{1}{\Gamma_s}\theta_g + \left(\frac{1}{\varepsilon}-1\right)\theta_s\right] \tag{16}$$

Using the same excess enthalpy function H = y + θ_g - 1 (note that θ_s is not included into H) defined before we find:

$$\frac{dH}{d\zeta} = \frac{d^2H}{d\zeta^2} + \underbrace{\left(\frac{1}{\mathrm{Le}_s}-1\right)\frac{d^2y}{d\zeta^2}}_{T2} + \underbrace{\left(\frac{1}{\Gamma_s}-1\right)\frac{d^2\theta_g}{d\zeta^2}}_{T3} + \underbrace{\left(\frac{1}{\varepsilon}-1\right)\frac{d^2\theta_s}{d\zeta^2}}_{T4} \tag{17}$$

When $\Gamma_s = \varepsilon = 1$ we recover a laminar free flame and when Le = 1 the enthalpy function is conserved. Otherwise, the equation for the enthalpy function H will have a positive or negative source term depending on the signs for the diffusion-like terms involving the nondimensional fuel fraction, gas and solid temperature distributions. The second term in the right hand side of the Eq. (17) - called here of source term T2 - is similar to the source/sink term of the Eq.(9), except that the Lewis number is now based on the thermal conductivity of the solid phase. This term accounts for the decrease of the mass diffusion thickness of the flame for a solid phase-based Lewis number Le_s larger than the unity, increasing the preheating of the nonreacted gas mixture. The third term - called source term T3 - accounts for the effect of the solid phase conduction on the gas phase nondimensional temperature distribution, due to the interfacial heat transfer. The interfacial heat transfer increase the width in the medium across which the gas phase temperature changes, when compared to the free flame. This effect can be understood as the effect that a variable volumetric heat source and loss would have in the gas phase temperature, even in the absence of any change in the medium thermal conductivity. The fourth term in the right hand side of the Eq. (17) - called source term T4 - accounts for the effect that the solid phase is immobile, and does not add to the advective energy flow. The overall result in the H distribution in the flame zone will depend on the relative magnitudes of these terms.

One Equation Model:

When the interfacial heat transfer parameter, responsible for the thermal contact between the continuous effective gas phase and the continuous effective solid phase, is sufficiently high, local thermal equilibrium between the phases may be safely assumed, i.e., θ_g.= θ_s = θ, and a one-medium model can be used. The energy equation for the one-medium model is obtained by adding up the energy equations for the gas (Eq. 10) and the solid (Eq. 11) phases and redefining the non-dimensional space coordinate by using the effective thermal conductivity in place of the effective phasic solid thermal conductivity. Thus, the one-medium model becomes:

$$\frac{dy}{d\zeta} = \left(\frac{1}{\mathrm{Le}\,\Gamma_e}\right)\frac{d^2y}{d\zeta^2} - \mathrm{Da}W \tag{18}$$

$$\frac{d\theta}{d\zeta} = \left(\frac{1}{\varepsilon}\right)\frac{d^2\theta}{d\zeta^2} + \mathrm{Da}W \tag{19}$$

and the H equation becomes:

$$\frac{dH}{d\zeta} = \frac{d^2H}{d\zeta^2} + \left(\frac{1}{\mathrm{Le}\Gamma_e}-1\right)\frac{d^2y}{d\zeta^2} + \left(\frac{1}{\varepsilon}-1\right)\frac{d^2\theta}{d\zeta^2} \tag{20}$$

where $\Gamma_e = \lambda_e/\lambda_g$ is the effective thermal conductivity ratio, where the effective thermal conductivity is $\lambda_e = \varepsilon\,\lambda_g + (1\text{-}\varepsilon)\,\lambda_s$. Mathematically, the one medium model differs from the free flame because the effective Lewis number is much greater than 1 and the porosity also appears dividing the heat diffusion term.

4. Results

Initially, results for adiabatic laminar free flames are reproduced as a way of validating the numerical code and for comparison with the results for combustion in porous media.

4.1. Laminar Free Flames

Equations (5) and (6) were solved numerically for the methane-air system. The boundary conditions are $\theta_g = 0$ and $y = 1$ for $\zeta \rightarrow -\infty$ and $\theta_g = 1$ and $y = 0$ for $\zeta \rightarrow +\infty$, with θ_g and y being constant in both situations. Table 1 shows the thermodynamic and transport properties used and the correspondent nondimensional parameters.

Table 1. Thermodynamic and transport properties for the gas phase and the correspondent nondimensional parameters.

Gas Phase Properties		
Φ	1	-
T_n	298	K
T_r	2197	K
E_a	141E3	J/mol
A_0	2.2E8	1/s
R_g	8.314	J/mol-K
u_n	0.65	m/s
λ_g	0.082	W/m-K
ρ_n	1.2127	kg/m^3
c_p	1452	J/kg-K
Q	50144	kJ/kg $_{\text{Fuel}}$
ν_F	1	-
a	0	-
Nondimensional Variables		
β	6.672	
α	0.8644	
Da	156.3	

The solution was obtained using a finite-volume method, with non-uniform, adapting grid and steps were taken to accelerate convergence to steady state. The flame speed (eigenvalue) was obtained from the overall mass balance. The algorithm was validated from the solution for a unit Lewis number and the experimental flame speeds for equivalence ratio of 1 and 0.5 for methane-air premixed combustion.

The calculated nondimensional gas temperature, fuel fraction, excess enthalpy (divided by its maximum value) and source term for equivalence ratio of 1 and Le = 2 are shown in Fig.(1). The preheat region begins in $\zeta = 387$ and the reaction region takes place in $393 < \zeta < 396$ (only a small region enclosing the flame is shown). The enthalpy function is everywhere positive (there is an excess enthalpy).

This figure also presents the distribution of the source term of Eq.(9) along the flame, showing that it is a positive source term for $388 < \zeta < 394$, causing an augmentation of the excess enthalpy function H, and is a negative source term for $394 < \zeta < 396$, causing a decrease of the excess enthalpy. Since both in the upstream and in the post flame regions the enthalpy is conserved, as expected for an adiabatic flame, the source term is zero in both the inlet and post-flame regions. Since the temperature and fuel fraction distributions are smooth and monotonic, the excess enthalpy is always positive and the areas under the positive and negative branches of the source term must add to zero. From Fig.(1) we note that even with excess enthalpy, the flame does not present superadiabatic temperatures. This is true also when Le >> 1, as it will be shown next.

Figure (2) shows the solution for equivalence ratio of 1 and Le = 0.5. As expected, the species diffusion is larger than the heat diffusion, beginning in $\zeta = 220$ while the preheat region begins in $\zeta = 226$. The reaction region takes place in $231 < \zeta < 234$. In this case, the enthalpy function is everywhere negative (there is a defect enthalpy). The source term is first negative and then positive, making the excess enthalpy function H decrease to a negative minimum value and then return to zero.

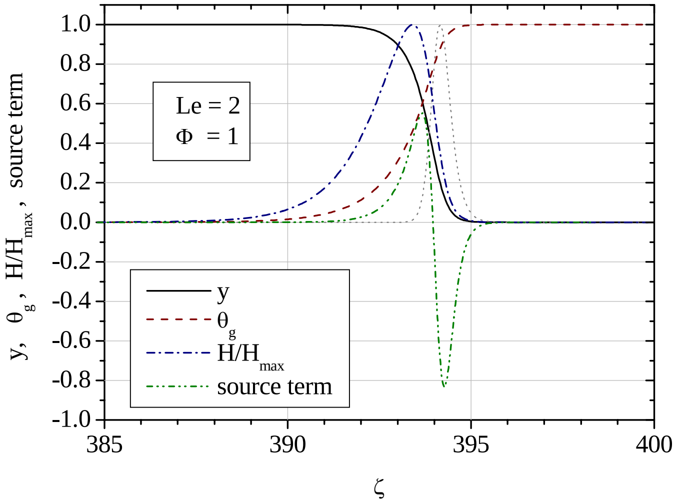

Figure 1. Nondimensional fuel fraction, gas temperature, excess enthalpy (divided by its maximum value) and source term distributions for a free flame with $\Phi = 1$ and $Le = 2$. The reaction rate is also shown as a thin dotted line.

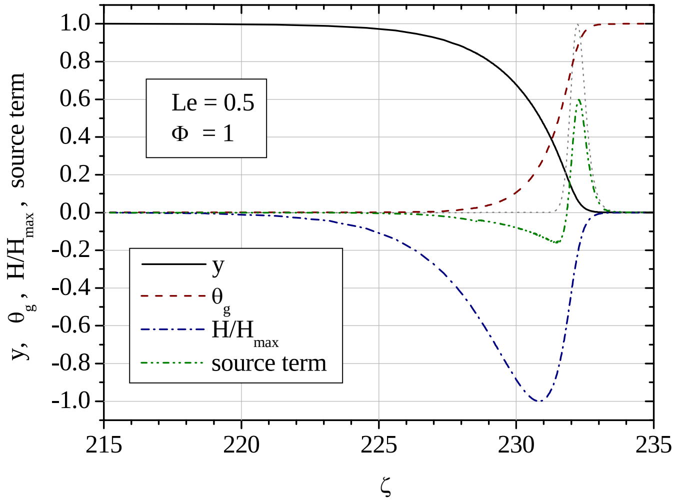

Figure 2. Nondimensional fuel fraction, gas temperature, excess enthalpy (divided by its maximum value) and source term distributions for a free flame with $\Phi = 1$ and $Le = 0.5$. The reaction rate is also shown as a thin dotted line.

Figure 3 shows the variation of the maximum enthalpy function H_{max} and the flame speed u_F with the Lewis number for $\Phi = 1$. Since the H function is conserved for a unit Lewis number, its value is zero when $Le = 1$. For $Le < 1$ the H function is always negative (defect enthalpy) and for $Le > 1$ it is always positive (excess enthalpy). The Lewis number also affects the flame speed, making it to decrease when there is defect enthalpy and to increase when there is excess enthalpy. This is due to the fact that with a wider thermal thickness more fuel is found inside the reaction region causing an augmentation of the reaction rate, consequently increasing the flame speed.

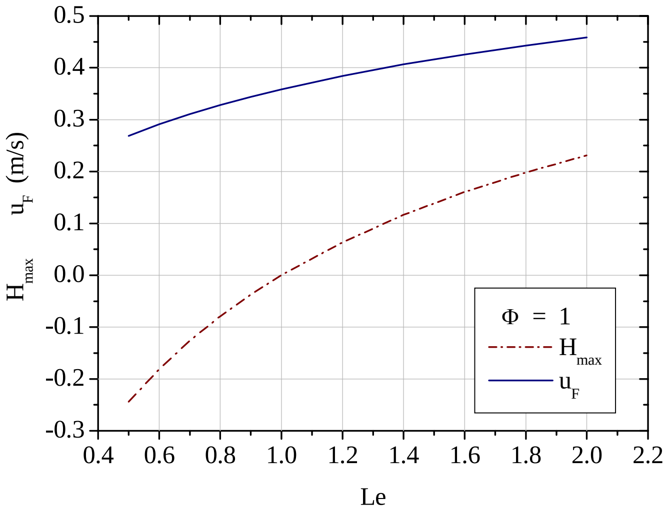

Figure 3. Variation of the maximum excess enthalpy H_{max} and the flame velocity u_F with the Lewis number for $\Phi = 1$.

4.2. Combustion in Porous Media

Equations (12), (13) and (14) were solved numerically following the same solution method described for the free-flame. The boundary conditions are $\theta_g = \theta_s = 0$ and $y = 1$ for $\zeta \rightarrow -\infty$ and $\theta_g = \theta_s = 1$ and $y = 0$ for $\zeta \rightarrow +\infty$, with θ_g , θ_s and y being constant in both situations.

Table 2 shows the transport and geometric properties of the solid phase and the corresponding nondimensional parameters used. The mean pore diameter is modeled as $D_p = (4\varepsilon/\pi)^{0,5}/(39.37 \text{ PPI})$ and the specific area between the phases as $S_{gs} = 66.69$ PPI, where PPI stands for pore-per-inch. An approximate value for the volumetric heat transfer coefficient is used. The solid phase properties are taken for a Zirconia burner (Möβauer et al., 1999). Note that the relatively high value of the thermal conductivity ratio leads to a relatively high value of solid phase-based Lewis number.

Table 2. Transport and geometric properties for the solid phase (Zirconia) and the nondimensional parameters used. The gas phase-based Lewis number is equal to unit.

Solid Phase Properties		
λ_s	5	W/m-K
ε	0.8	-
PPI	10	ppi
S_{gs}	667	m^2/m^3
L_q	0.10	m
D_p	2.56E-3	m
hv	60E+3	W/m^3K
Nondimensional Variables		
Le_s	61	
Γ_s	61	
N	0.227	
Re_D	9.884	

Figure (4) shows the nondimensional fuel fraction, gas and solid temperatures and excess enthalpy distributions for a premixed flame within a porous media with the equivalence ratio equal to unit. The nondimensional gas temperature presents a peak that is 10% higher than the adiabatic flame temperature (the gas temperature is 230K higher than the adiabatic flame temperature). The thermal flame thickness is wider than the fuel fraction thickness as a result of the large effective Lewis number. The enthalpy function presents an excess everywhere along the flame.

Figure (5) presents the variation along the flame of the last three terms of Eq. (17), repeated below for easier reference. The dotted lines are the nondimensional gas temperature and fuel fraction distributions. Since the solid is more conducting than the gas phase, Le_s is larger than 1 and the prefactor $(Le_s^{-1}-1)$ is a negative number. The term T2 always cause an excess enthalpy in the flame region. Since the conductivity ratio Γ_s is greater than 1, the prefactor $(\Gamma_s^{-1}-1)$ is a negative number and, given the sign od $d^2\theta/d\zeta^2$, the term T3 will cause a defect enthalpy. As the porosity is always smaller than 1 the prefactor ($\varepsilon^{-1} - 1$) will always be positive and the term T4 will always cause an excess enthalpy.

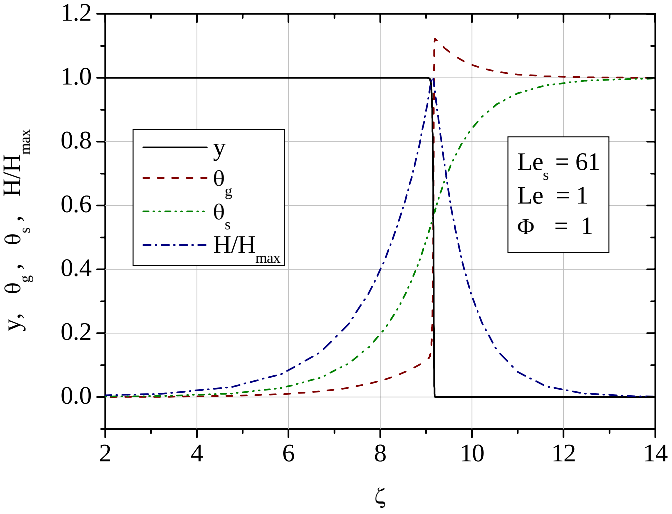

Figure 4. Nondimensional gas and solid temperatures, fuel fraction profile and excess enthalpy distribution (divided by its maximum value) for a flame within a porous media with $\Phi = 1$, $Le = 1$ and $Le_s = 61$.

We note that the second (T2) and third (T3) terms dominate the source term, being the second (always in modulus) larger than the third. Also note that the difference between T2 and T3 is of the order of 0,1% of their absolute values. The fourth term (T4) has only a small effect in the regions far in the post-flame zone. Although not clear in Fig.(5), because of the clipping in the ζ axis to present the flame zone only, the positive and negative areas under the total source term distribution also add up to zero. The excess enthalpy is therefore, primarily a Γ_s effect both in T2 and T3. An increase in the gas Lewis number, would increase even more the effect of the T2 term. A reduction in the Lewis number would reduce the value of the T2 term when compared to the T3 term, leading, when smaller enough, to a defect enthalpy.

$$\frac{dH}{d\zeta} = \frac{d^2H}{d\zeta^2} + \underbrace{\underbrace{\left(\frac{1}{Le_s}-1\right)\frac{d^2y}{d\zeta^2}}_{T2} + \underbrace{\left(\frac{1}{\Gamma_s}-1\right)\frac{d^2\theta_g}{d\zeta^2}}_{T3} + \underbrace{\left(\frac{1}{\varepsilon}-1\right)\frac{d^2\theta_s}{d\zeta^2}}_{T4}}_{Total-Source-Term}$$

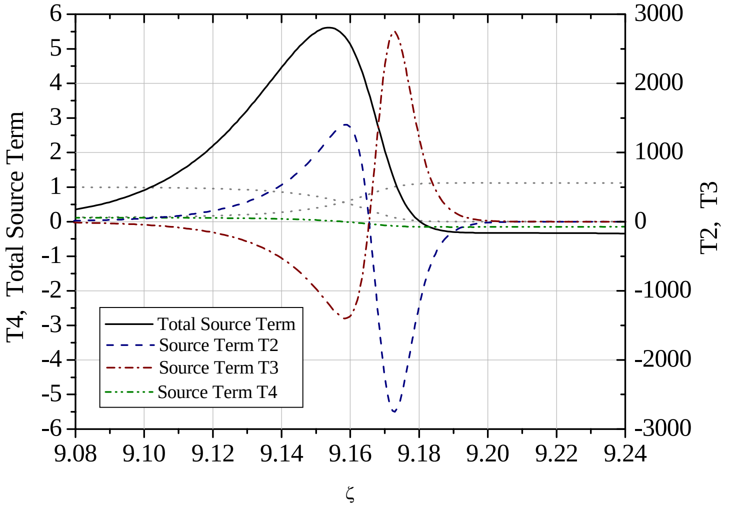

Figure 5. Variation of the three source terms T2, T3 and T4 and the total source term of Eq. (17) along the flame for a flame within a porous media with $\Phi = 1$ and $Le_s = 61$. The distributions of y and θ_g are also shown as thin dotted lines.

Figure 6 shows the variation of the maximum enthalpy function H_{max} and the flame speed u_F with the Lewis number for $\Phi = 1$. H_{max} is always positive, varying from 1.13 to 2.10 when Le_s rises from 61 to 365. The flame speed increased from 0.65 m/s to 0.95 m/s in the same range of Le_s.

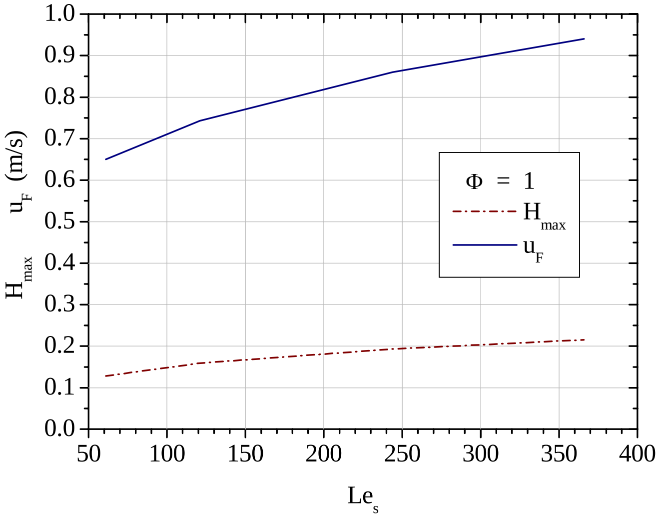

Figure 6. Variation of the maximum excess enthalpy H_{max} and the flame velocity u_F with the solid Lewis number Le_s for $\Phi = 1$.

4.3. Excess Temperature

Figure 7 shows the variation of the excess enthalpy function with the nondimensional fuel concentration for laminar free flames with Le = 2 and 100 and for premixed flames within a porous medium with $Le_s = 61$ and 244. When the nondimensional fuel concentration is equal to unit, i.e., when no fuel has yet been consumed, all flames present an almost vertical excess enthalpy curve. This is due to the enhanced preheating of the gas flow caused by its low mass diffusivity (Le > 1). The cold reactants receive energy by conduction from the reaction region achieving an excess enthalpy before entering the flame region. For a laminar free flame, as the nondimensional fuel fraction decreases, the excess enthalpy increases and then decreases reaching zero when all fuel is consumed. The adiabatic limit for the excess enthalpy is also shown. This adiabatic limit is found when $\theta_g = \theta_{ad} = 1$ is placed in the H equation giving H = y. For points that lie above this limit, i.e., an H function greater than y, the local nondimensional temperature reaches values above the adiabatic temperature. This region is identified in Fig.(7) as the superadiabatic region. As expected, laminar free flames never cross this limit even for very high Lewis numbers and consequently cannot reach temperatures over the adiabatic flame temperature. For flames within porous media, the adiabatic limit is crossed by the H function in y = 0.13 for $Le_s = 61$ (typical of Zirconia burners) and in y = 0.19 for $Le_s = 244$ (typical of Silicon Carbide burners), meaning the existence of excess gas phase temperatures above the adiabatic temperature. The maximum gas temperature occurs when the H function sharply drops at y = 0. This corresponds to $\theta_g = 1.13$ and 1.19 for $Le_s = 61$ and 244 respectively. The H line is almost flat as a result of the sharp decrease in y when compared to θ_g and θ_s .

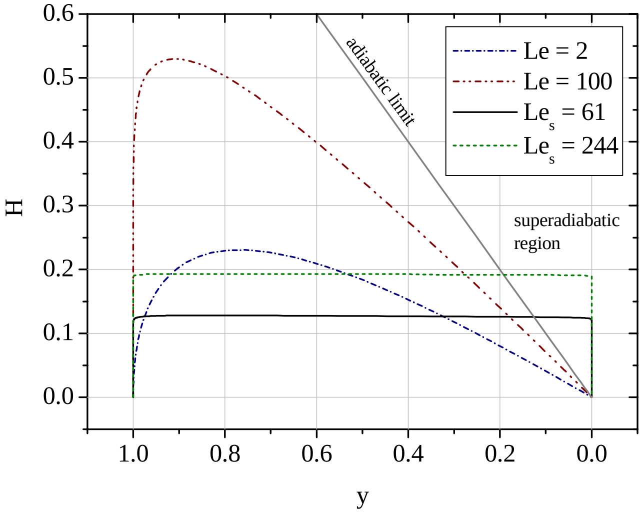

Figure 7. Variation of the excess enthalpy function H with the nondimensional fuel concentration y.

Figure 8 shows the behavior of H as a function of y for three different values of Le and $\Gamma_s = 61$. As the gas phase-based Lewis number decreases, a region of defect enthalpy appears as a result of the T3 term prevailing over the T2 term. However at the end of the reaction region the temperature still reaches an excess value. In this region, the T2 term prevails again. Also, the lower Lewis number leads to higher maximum enthalpy in the flat region of the curve at y = 0, which results in higher superadiabatic flame temperatures. This seems to be caused by the combined effects of the high solid conductivity and finite interfacial heat transfer coefficient. We continue to work to better explain this effect and intend to report this in a next opportunity.

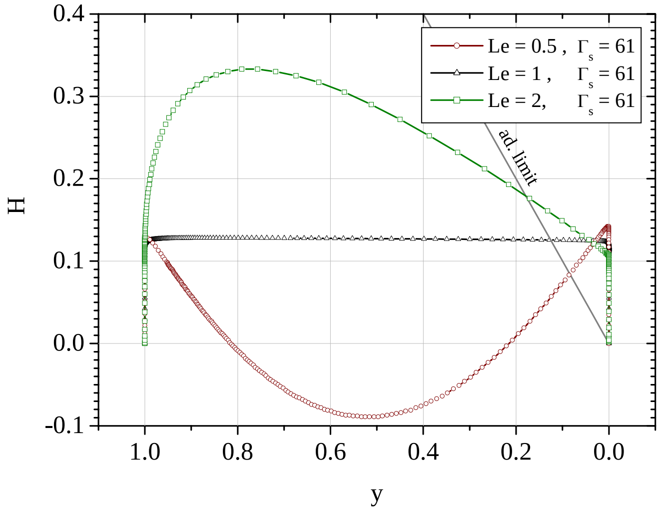

Figure 8. Effect of the gas phase-based Lewis number Le on the excess enthalpy function H for a porous media with $\Gamma_s = 61$.

Figure 9 shows the variation of the superadiabatic flame temperature T_{sup} with the solid phase-based Lewis number. The temperature of the gas exceeds the adiabatic flame temperature for a methane/air flame with $\Phi = 1$ (T_{ad} = 2197,5°C) in 240°C for $Le_s = 61$ (typical value for zirconia burners) and in 390°C for $Le_s = 365$ (typical value for metalic burners). For $\Gamma_s = 61$, the maximum temperature reached by the gas phase for Le = 0.5 was 2510°C and for Le = 2 was 2466°C.

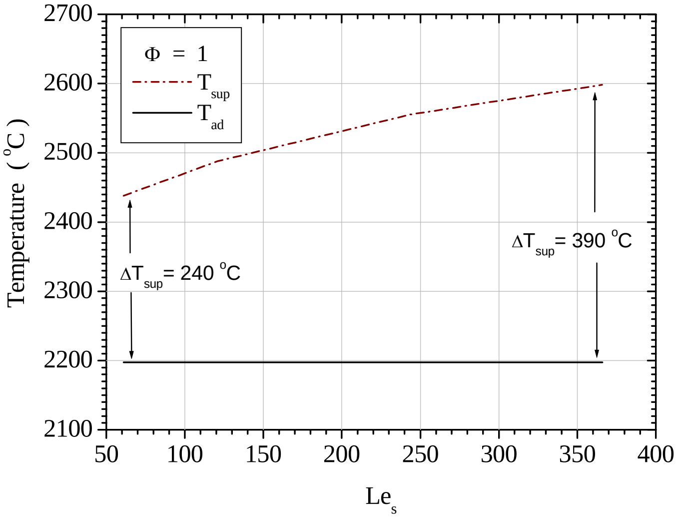

Figure 9. Variation of the superadiabatic temperature with the solid phase-based Lewis number Le_s.

5. Conclusions

The excess enthalpy in free flames and in flames within porous media is analyzed to access the amount of excess temperature above adiabatic temperature originated by the presence of the porous matrix and the factors that affect it. This analysis is based on the excess enthalpy function previously defined in the literature. The results show that:

- For adiabatic laminar free flames, for $Le > 1$, the excess enthalpy function is always larger than 1, as expected, without, however, presenting gas temperatures above the adiabatic flame temperature. For $Le < 1$, the excess enthalpy function is always smaller than 1.
- For the combustion within a porous media, for $Le_s > 1$, there is excess enthalpy and a region of gas temperatures above the adiabatic temperature, i.e., there is a region of excess temperature. This region is identified in a plot of H against the nondimensional fuel fraction y.
- In the source term for the H equation for the porous medium, the contribution of the last term (T4) is negligible in the flame zone. This term accounts for the effect that the solid phase is immobile. The behavior of H is controlled by the interplay between the T2 and T3 terms. The T2 term accounts for the decrease of the mass diffusion thickness of the flame when the solid phase-based Lewis number Le_s is larger than one. It depends on the gradients of the nondimensional mass fraction. The T3 term accounts for the effect of the solid phase conduction on the gas phase nondimensional temperature distribution, due to the interfacial heat transfer. It depends on the gradients of the nondimensional solid temperature. The excess enthalpy is, therefore, primarily a function of Γ_s.
- The necessary condition for reaching gas temperatures above the adiabatic temperature is $Le_s > 1$ (the product of the gas Lewis number Le and the thermal conductivity ratio Γ_s being larger than 1) combined to a finite interfacial heat transfer coefficient. The first is responsible for the enhanced thermal diffusion when compared to the mass diffusion and the second is responsible for a volumetric heating of the gas phase then increasing the excess enthalpy.

The analysis should be further extended to verify the role of Le in the maximum excess temperature. A parametric analysis of the effect of interfacial heat transfer and equivalence ratio should be performed to identify the behavior of the threshold points of the superadiabatic temperature zone. Finally, a closed form analytical solution based on assymptotic analysis is being developed to readily quantify the effect of the various parameters in the amount of excess tempeature. This will be reported in a next opportunity.

6. Acknowledgement

The authors acknowledge the support of the FINEP/RedeGasEnergia through a CTPETRO grant. The comments by Dr. Ricardo Serfaty (CENPES-PETROBRÁS) are also greatly appreciated.

7. References

Babkin, V.S., Wierzba, I. and Karim, G.A., 2003, “The Phenomenon of Energy Concentration in Combustion Waves and Its Applications”, Chemical Engineering Journal, Vol.91, pp. 279-285.

Echigo, R., 1991, “Radiation Enhenced/Controlled Phenomena of Heat and Mass Transfer in Porous Media”, ASME/JSME Thermal Engineering Proceedings, Vol.4, pp. 21-32.

Fu, x., Viskanta, R. and Gore, J.P., 1998, “Measurement and Correlation of Volumetric Heat Transfer Coefficients of Cellular Ceramics”, Experimental Thermal and Fluid science, Vol.17, pp. 285-293.

Hardesty, D.R. and Weinberg, F.J., 1974, “Burners Producing Large Excess Enthalpies”, Combustion Science and Technology, Vol.8, pp. 201-214.

Howell, J.R., Hall, M.J. and Ellzey, J.L., 1996, “Combustion of Hidrocarbon Fuels Within Porous Inert Media”, Progress in Energy and Combustion Science, Vol.22, pp. 121-145.

Hsu, J.R., Matthews, R. D., 1993, "The Necessity of Using Detailed Kinetics in Models for Premixed Combustion Within Porous Media", Combustion and Flame, Vol. 93, pp.457-466.

Min, D.K. and Shin, H.D., 1991, “ Laminar Premixed Flame Stabilized Inside a Honeycomb Ceramic”, International Journal of Heat and Mass Transfer, Vol.34, No.2, pp. 341-356.

Mittal R., Gore, J.P. and Viskanta, R., 1997, "A Study of the Structure of Submerged Reaction Zone in Porous Ceramis Radiant Burners", Combustion and Flame, Vol. 111, pp. 175-184.

Möβauer, S., Pickenäcker, O., Pickenäcker K. and Trimis, D., 1999, “Application of the Porous Burner Technology in Energy- and Heat-Engineering”, V International Conference on Technologies for a Clean Air Environment, Lisbon.

Oliveira, A.A.M. and Kaviany, M., 2001, “Nonequilibrium in the Transport of Heat and Reactants in Combustion in Porous Media”, Progress in Energy and Combustion Science, Vol.27, pp. 523-545.

Saharaoui, M. and Kaviany, M., 1994, “Direct Simulation vs Volume-Averraged Treatment of Adiabatic, Premixed Flame in a Porous Medium”, International Journal of Heat and Mass Transfer, Vol.17, No.18, pp. 2817-2834.

Wichman, I.S. and Vance, R., 1997, “A Study of One-Dimensional Laminar Premixed Flame Annihilation”, Combustion and Flame, Vol.110, pp. 508-523.

Williams, F., 1985, "Combustion Theory the Fundamental Theory of Chemically Reacting Flow Systems", Perseus Publishing; 2nd edition.

Yoshizawa, Y., Sazaki,K. and Echigo, R., 1988, “Analytical Study of the Structure of Radiation Controlled Flames”, International Journal of Heat and Mass Transfer, Vol.31, No.2, pp. 311-319.

8. Nomenclature

a	temperature exponent in the reaction rate equation
A	pre-exponential factor
c_p	specific heat
D	mass diffusivity
Da	Damköhler number
D_p	mean pore diameter
E_a	activation energy
h	convection coefficient $h = S_{gs}(Nu\lambda_{g,m}/D_p)$
H	excess enthalpy function $H = y + \theta - 1$
Le	Lewis number $Le = \lambda/\rho D c_p = \alpha_g/D$
Le_s	modified Lewis number $Le_s = Le\Gamma_s$
L_q	lengh of the burner
N	heat transfer between the phases parameter
Nu	Nusselt number
Q	chemical heat release
R_g	universal gas constant
Re_D	Reynolds number $Re = \rho u D_p/\mu$
S_{gs}	specific area between the phases
T	temperature
u	flow velocity
W	non dimensional reaction rate
y	reduced fuel mass fraction $y = Y_F/Y_{F,n}$
Y_F	fuel mass fraction

Greek Symbols

α	enthalpy ratio $\alpha = 1 - T_n/T_r$ or thermal diffusivity
β	Zeldovich number $\beta = \alpha(E_a/R_gT_r)$
ε	solid matrix porosity
λ	thermal conductivity
ν_F	fuel stoichiometric coefficient
ρ	density
μ	viscosity
θ	nondimensional normalized temperature $\theta = (T_g - T_n)/(T_r - T_n)$
Φ	equivalence ratio
Γ_s	conductivity ratio $\Gamma_s = \lambda_s/\lambda_g$
ζ	spatial coordinate $\zeta = \int_0^x \frac{\rho_n u_n c_p}{\lambda_s} dx$

Subscripts

e	effective
g	gas phase
i	ignition
m	molecular
max	maximum
n	non-reacted
r	reacted
s	solid phase